ACS Chemical Neuroscience

pubs.acs.org/chemneuro

Research Article

Characterization of the Novel P2X7 Receptor Radioligand [^{3}H]JNJ-64413739 in Human Brain Tissue

Jens D. Mikkelsen,* Sanjay S. Aripaka, Sif Kaad, Burcu A. Pazarlar, Lars Pinborg, Bente Finsen, Andrea Varrone, Benny Bang-Andersen, and Jesper F. Bastlund

Cite This: *ACS Chem. Neurosci.* 2023, 14, 111−118

Read Online

ACCESS | Metrics & More | Article Recommendations

ABSTRACT: Radioligands targeting microglia cells have been developed to identify and determine neuroinflammation in the living brain. One recently discovered ligand is JNJ-64413739 that binds selectively to the purinergic receptor P2X7R. The expression of P2X7R is increased under inflammation; hence, the ligand is considered useful in the detection of neuroinflammation in the brain. [^{18}F]JNJ-64413739 has been evaluated in healthy subjects with positron emission tomography; however, the in vitro binding properties of the ligand in human brain tissue have not been investigated. Therefore, the purpose of this study was to measure B_{max} and K_d of [^{3}H]JNJ-64413739 using autoradiography on human cortical tissue sections resected from a total of 48 patients with treatment-resistant epilepsy. Correlations between the specific binding of [^{3}H]JNJ-64413739 with age, sex, and duration of disease were explored. Finally, to examine the relationship between P2X7R and TSPO availability, specific binding of [^{3}H]JNJ-64413739 and [^{123}I]CLINDE was examined in the same tissue. The binding was measured in both cortical gray and subcortical white matter. Saturation revealed a K_d (5 nM) value similar between gray and white matter but a larger B_{max} in the white than in the gray matter. The binding was completely displaced by the cold ligand and structurally different P2X7R ligands. The variability in saturable binding among the samples was found to be 38% in gray and white matter but was not correlated to either age, sex, or the duration of the disease. Interestingly, there was no significant correlation between [^{3}H]JNJ-64413739 and [^{123}I]CLINDE binding. These data demonstrate that [^{3}H]JNJ-64413739 is a suitable radioligand for evaluating the distribution and expression of the P2X7R in the human brain.

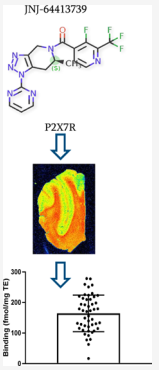

KEYWORDS: *P2X7, autoradiography, purinergic receptor, epilepsy, TSPO, neuroinflammation*

INTRODUCTION

The homomeric P2X7 receptor (P2X7R), a member of the purinergic family of receptors, is an adenosine triphosphate (ATP)-gated ion channel expressed predominantly in macrophages and monocytes in the periphery, and in microglia and astrocytes in the central nervous system (CNS).[1] Under normal physiological conditions, extracellular ATP concentrations are below the threshold required for P2X7R activation, but under some pathological conditions, ATP levels can reach sufficiently high levels to activate the receptor.[2] Accordingly, mounting evidence point to the important role of P2X7R in multiple diseases in the CNS, particularly those involving neuronal cell death and regeneration.[1−4]

P2X7R expression has been reported in almost all cellular lineages constituent of the brain tissue, including neurons, astrocytes, microglia, and oligodendrocytes.[5] While the expression and function of P2X7R in microglia and oligodendrocytes are well established, its presence in neurons is more controversial.[6,7] The expression of P2X7R is variable, and its presence and functions are often studied under various pathological conditions and not the steady state.[8] Despite the observation that under basal conditions, ATP concentrations are lower than those required for P2X7R activation, the receptor has been considered involved in several physiological and pathophysiological events including neurotransmitter release,[9−11] microglial activation, migration, and proliferation.[10−12] Of special interest, P2X7R has been reported to be increased in the temporal cortex tissue from drug-refractory temporal lobe epilepsy patients.[40]

The best-characterized activity of P2X7R is its role in ATP-induced interleukin 1b (IL-1b) and IL-18 release from macrophages and microglia that have been primed with substances such as bacterial endotoxin.[13,14] Hence, P2X7R is considered to have a pivotal role in inflammatory conditions in the brain.

Reliable methods to measure neuroinflammation in the living brain are highly needed, and PET imaging is a key technology providing the opportunity to image specific molecules with medium special resolution.[15] Translocator

Received: September 20, 2022
Accepted: November 9, 2022
Published: December 19, 2022

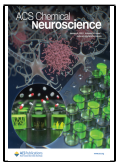

protein (TSPO) is currently recognized as the prime target, yet there are important limitations to the applicability of TSPO radioligands[16] which mostly stem from suboptimal cellular specificity and genetic polymorphism that affect the binding of most TSPO ligands.[15] As an alternative to TSPO, P2X7R is considered one of the most attractive targets for second-generation radioligand development for neuroinflammation. Several PET ligands targeting P2X7R, for example, [^{11}C]-GSK1482160,[17] [^{11}C]JNJ-54173717,[18] [^{18}F]JNJ-64413739,[19−22] [^{18}F]EFB,[23] and [^{18}F]PTTP,[24] have been developed and evaluated in a preclinical setting. To our knowledge, only [^{18}F]JNJ-64413739,[21] [^{11}C]JNJ-54173717,[25,26] and [^{11}C]SMW139[27] have hitherto been used for in vivo quantification of the P2X7R expression in the human brain, but these radioligands have demonstrated variable kinetics and specificity. [^{18}F]JNJ-64413739 has been one of the most promising radioligands, initially evaluated in nonhuman primates[20] and recently validated in healthy individuals with positron emission tomography.[21,22] [^{18}F]JNJ-64413739 binds to P2X7R in low nM concentrations and in healthy humans and showed good test−retest reliability and uptake consistent with the distribution of P2X7R.[22] However, these studies have been conducted on only a few individuals and we still need data from larger cohorts to know more about variations in expression in the population, and we need to see analysis in patients. Despite the initial in vivo evaluation in humans, to our knowledge, the binding of JNJ-64413739 in human brain tissue in vitro has not been validated. The aim of this study was to examine the binding properties of [^{3}H]JNJ-64413739 using autoradiography on human brain sections. Cortical resections of the temporal lobe from patients neurosurgically treated for treatment-resistant epilepsy were used. This tissue is collected and frozen within a short period of time with minimal degradation of proteins as well as other molecules. A secondary objective was to analyze the between-subject variability in the specific binding of [^{3}H]JNJ-64413739 and its correlation to clinical and demographic data. Furthermore, we compared the binding of [^{3}H]JNJ-64413739 with the binding of the TSPO radioligand [^{123}I]CLINDE as a marker of glial cell density in the brain.

RESULTS

Frozen sections of temporal cortical resections obtained from patients with temporal lobe epilepsy were used in this investigation to validate the binding properties of [^{3}H]JNJ-64413739 to P2X7R. High specific binding was observed in both the gray and subcortical white matter (Figure 1). In some specimens, a slightly stronger binding was observed in the most superficial subcortical white matter adjacent to the gray matter, in particular, in those individuals with a high level of binding.

Physiochemical Properties and Qualitative Observations. Because binding of [^{3}H]JNJ-64413739 to frozen brain sections using autoradiography has not been reported before, we first performed some pilot experiments to determine the optimal physiochemical conditions for the autoradiographical procedure. First, various compositions of the incubation buffers and pH levels were investigated, and second, comparative experiments were performed to define the optimal temperature and time in the incubation and in the washing steps. The optimal temperature for incubation was found to be close to room temperature, as colder temperatures reduced binding significantly and higher temperatures up to 37 °C did not yield higher binding (not shown). Increasing incubation

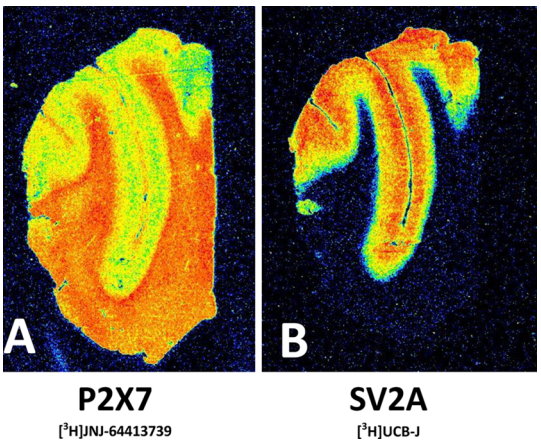

Figure 1. Representative autoradiograms of adjacent sections of the temporal cortex incubated with [^{3}H]JNJ-64413739 for P2X7R (A) and [^{3}H]UCB-J for synaptic vesicle protein 2A (SV2A) (B). SV2A is found exclusively in the gray matter, and with that reference, P2X7R binding is distributed in both the white and gray matter.

times were evaluated, and the optimal time frame was found to be between 30 min and 4 h. The washing procedure was also validated in terms of temperature and time, and extensive washing for 15 min in ice-cold preincubation could wash off the nonspecific binding to the tissue most effectively. Based on these initial validation experiments, autoradiography was carried out with incubation at room temperature for 2 h, and the washing procedures were performed for 15 min at 4 °C.

Repeated analysis on several samples in the same experiment produced an intra-assay variation of 1.5%, and successive experiments with the same samples revealed an interassay variation of 2%.

The binding was found to be rather dense throughout both gray and white matter. As shown, the binding was strong in the temporal cortex and ubiquitously distributed in both compartments (Figure 1A). For comparison of a more precise delineation of the gray matter, we carried out binding studies for SV2A on adjacent sections (Figure 1B). In the neocortical tissue, higher binding intensity was observed in the subcortical white matter compared to the gray matter (Figure 1).

Saturation and Displacement Experiments. Based on the developed and validated protocol, saturation experiments were performed. Binding of [^{3}H]JNJ-64413739 reached saturation in both white and gray matter (Figure 2). The saturation profile indicated one specific and high-affinity binding site. The binding was saturable in concentrations up to 100 nM in both compartments, and displacement could be achieved with the nonspecific binding representing a straight line (Figure 2). The analysis was carried out separately in white and gray matter and for the combined compartments. Full saturation was achieved, and the K_d for the two was similar and calculated to be around 7 nM. B_{max} in the white matter was ∼40% higher than B_{max} in the gray matter (Figure 2).

A displacement study shown in Figure 3 was carried out using three P2X7R antagonists JNJ-47965567, JNJ-64413739, and Lu AF27139, which were added to the incubation medium to assess binding specificity and displacement properties. All three ligands were able to reach the full displacement of [^{3}H]JNJ-64413739 at concentrations up to 1 μM. The calculated best fit for IC_{50} was 23 nM for JNJ-64413739, 68 nM for JNJ-47965567, and 89 nM for Lu AF27139, respectively (Figure 3).

https://doi.org/10.1021/acschemneuro.2c00561
ACS Chem. Neurosci. 2023, 14, 111−118

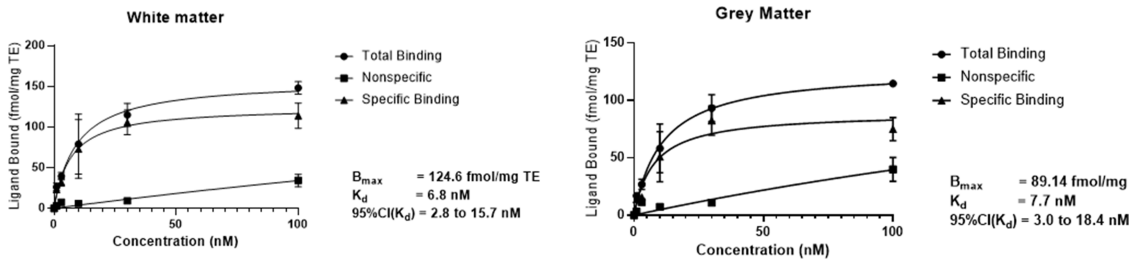

Figure 2. Saturation binding [^{3}H]JNJ-64413739 in the human temporal cortex. [^{3}H]JNJ-64413739 demonstrated concentration-dependent binding to the sections with a saturable specific binding that is similar in white (left) and gray (right) matter. Data are expressed as mean ± SD from three replicates per data point.

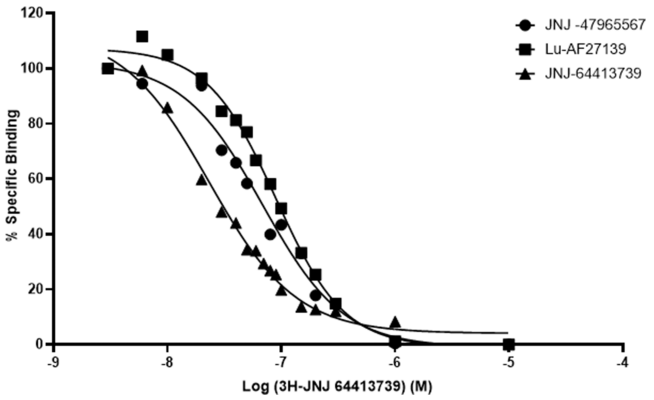

Figure 3. Displacement of [^{3}H]JNJ-64413739 in human brain sections with JNJ-64413739, JNJ-47965567, and Lu AF27139. Calculated best fit for IC_{50} was 23 nM (JNJ-64413739, 95% Conf interval, 17−29 nM), 68 nM (JNJ-47965567, 95% Conf interval, 48−88), and 89 nM (Lu AF27139, 95% Conf interval, 77−101 nM). Data are expressed as means from three replicates per data point.

Gray Matter and White Matter Binding. To compare the data from the cohort of involved specimens, we analyzed the binding level in the two compartments in each specimen. The binding pattern of [^{3}H]JNJ-64413739 in the human cortex tissue showed a polarized distribution of P2X7R. Across all tissue sections, the average specific binding was about 2-fold higher ($P < 0.001$) in the subcortical white matter than in the gray matter (Figure 4A). The variability measured as the standard deviation relative to the mean was determined to be 38% and was the same in white and gray matter.

Because of the large variability of specific binding in gray and white matter, for each patient, we examined the correlation of the specific binding in the two compartments. A strong correlation in specific binding between white and gray matter was observed ($r = 0.8$; $P < 5 \times 10^{-12}$) (Figure 4B).

Relationship between Specific Binding and Age, Sex, and Disease Duration. The age of the individuals at the time of surgery in the cohort spans from young adults around 18 years to older adults around 60 years. The disease duration in terms of years each patient had epilepsy-related symptoms ranged between 4 and 59 years. No statistically significant correlation was observed between the specific binding of [^{3}H]JNJ-64413739 in gray or white matter and age at the time of surgical treatment (Figure 5A) or the disease duration (Figure 5B). Furthermore, no sex differences were observed (not shown).

It should be noted that the time kept in the freezer had no effect on the binding in the tissues (not shown).

Comparison to TSPO Binding. The variation in the binding levels could reflect different stages of microglia activation independent of age and disease. It was therefore of interest also to correlate the radioligand binding with another radioligand [^{123}I]CLINDE known to bind to TSPO.[29] Because the level of [^{123}I]CLINDE binding is dependent on a genetic polymorphism,[16] specimens included to be compared to [^{3}H]JNJ-64413739 binding were limited to the 24 subjects that were high TSPO binders. Furthermore, because TSPO is equally distributed in white and gray matter, we analyzed the binding in the entire tissue section displaying high [^{123}I]-CLINDE binding. Analyzing the level of [^{123}I]CLINDE binding in the patients showed no correlation between binding

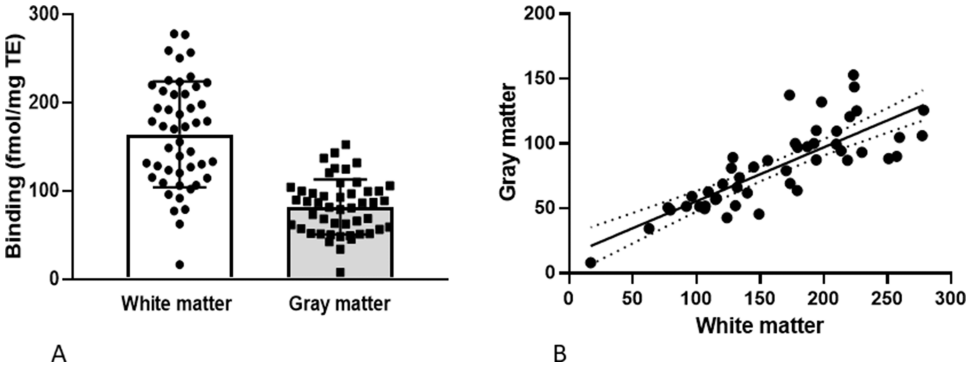

Figure 4. Levels of the binding capacity of [^{3}H]JNJ-64413739 in the white and gray matter in the cohort of 48 specimens. Data are expressed as a single data point from each patient. (A) Direct comparison of binding capacity in white and gray matter in the same tissue section ($P < 0.001$ between the two compartments). (B) Same data, but correlating the level in the two compartments from each patient. Very strong correlation between the two binding levels in the two areas are shown ($r = 0.80$; $P = 5.7 \times 10^{12}$).

https://doi.org/10.1021/acschemneuro.2c00561
ACS Chem. Neurosci. 2023, 14, 111−118

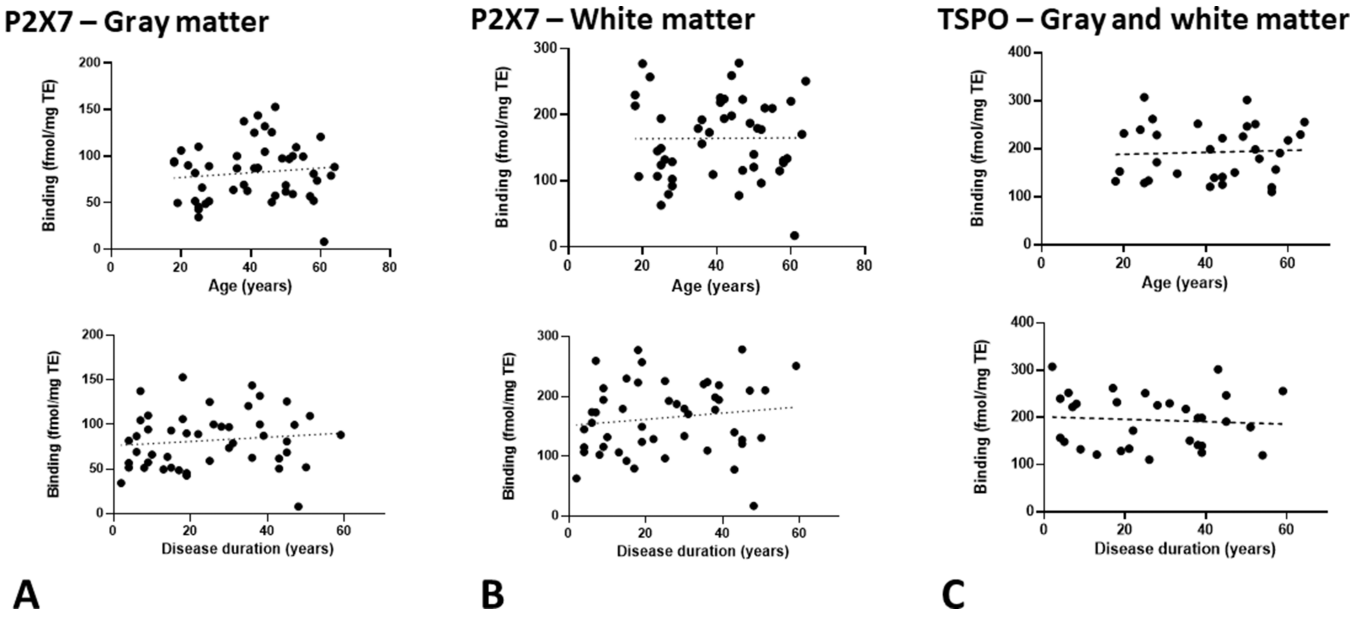

Figure 5. Correlation of binding of [^{3}H]JNJ-64413739 and [^{123}I]-CLINDE to age and disease duration. (A) Individual data points for [^{3}H]JNJ-64413739 binding for each patient in the white matter. (B) Individual data points for [^{3}H]JNJ-64413739 binding in the same patients in the gray matter. (C) Individual data points for [^{123}I]-CLINDE in relation to age and disease duration for patients with high TSPO binding. There was no association between binding and age or the disease duration in any of these data sets.

levels and neither age of the patients at the time of surgery nor the disease duration (Figure 5C).

No significant correlation was observed between [^{3}H]JNJ-64413739 and [^{123}I]CLINDE binding among the patients included (Figure 6). Given that both radioligands bind to glia

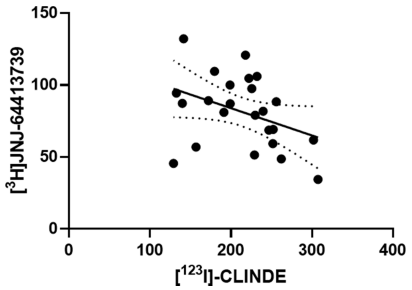

Figure 6. Correlation between the binding of [^{3}H]JNJ-64413739 and [^{123}I]-CLINDE in adjacent sections of the temporal cortex from patients with epilepsy. Only patients with high binding genetic polymorphism was included in this analysis. It should be noted that there is a tendency toward a negative correlation between the binding potentials.

cells, we would expect a positive correlation between the two binding capacities for the two ligands in the same patients, but interestingly, a rather negative correlation was seen, although not reaching significance (P = 0.06).

DISCUSSION

This study examined the in vitro binding properties of the P2X7R radioligand [^{3}H]JNJ-64413739 in the human temporal cortex. The ligand binds to P2X7R with high affinity as demonstrated by saturation and displacement experiments. In repeated experiments, K_d was measured to be around 5 nM. Full saturation was achieved around 30 nM, and this concentration was used to determine the binding potential in the tissues.

Radioligand binding to a given protein may not always reflect the concentration of a protein detected by immunoassays or by reporter assays. This is emphasized by the observation that significant binding is detected in the white matter in humans as reported here, but not by immunolocalization in rodents.[32]

Autoradiography allows quantitative and qualitative estimation of binding in subcompartments of the brain. Here, we report the presence of P2X7R binding in both white and gray matter. Specific binding was higher in the white matter than in the gray matter. While the expression of P2X7R is well documented in microglia and astrocytes, it is more controversial in neurons,[6,7] so the differences in binding might be explained by relative differences in cellular compositions between gray and white matter. In agreement with our finding, high uptake was found in subcortical white matter in a first-in-human PET study with [^{18}F]JNJ-64413739.[21] Furthermore, there is evidence to support the presence of P2X7R protein and mRNA in white matter, which is mostly attributed to astrocytes and oligodendrocytes,[33−35] and we assume that the ligand binds to these cell types in this compartment.

We find subject variability in binding to be around 38% in both white and gray matter. The measurements ranged among samples by more than 15-fold from the lowest to the highest. Because the interassay variation was less than 2%, the variability cannot be explained by the assay but must be explained by the samples or the population. This is important when studying larger cohorts for in vivo binding as it would be expected that P2X7R binding would display large variability in the brain also under baseline conditions.

Several mechanisms underlying this variability should be considered. Because the binding in white and gray matter was strongly correlated, it would imply that the expression of P2X7R is not different between specific cell types dominating each of the compartments. This indicates that the mechanisms behind the variability are more dependent on different

https://doi.org/10.1021/acschemneuro.2c00561
ACS Chem. Neurosci. 2023, 14, 111−118

conditions in the expression of the gene encoding P2X7R in the tissue rather than different mechanisms of P2X7R expression in cellular subtypes.

Similar to other members of the P2X family, the P2X7R subunit has two transmembrane domains linked by a large extracellular domain and these subunits present a dolphin-shaped structure with the transmembrane helices and the extracellular region similar to the tail and the body, respectively.[36] It is speculated that the binding site could be modulated in a manner that influences the binding properties as seen for other receptors, but so far, no evidence has been reported.

Another possibility is that the variation stems from differences in the transcription and/or translation of the gene. The human P2X7R protein is a 595 amino acid protein encoded by the P2RX7 gene located on chromosome 12 (12q24.31 locus) spanning 53,733 bases.[37] Alternative splicing takes place during gene transcription and may give rise to at least seven different splice variants of P2X7R.[38] The splice variants that are functionally tested, one of them lacking the C-terminal part is widely expressed in the brain and displays a lower functional activity for BzATP and other modulators,[38] so it cannot be excluded that the variability in protein expression may contribute for the variability in binding reported here. Hence, testing the specificity of [^{3}H] or [^{18}F] JNJ-64413739 across known splice variant products would be interesting in brain tissue from animals with different splice variants of P2X7R.

The P2X7R expression has been shown to be increased in several brain regions including the neocortex in animal models of prolonged seizure activity including status epilepticus, such as systemic kainic acid and intra-amygdala injections of kainic acid,[8,32,41] or systemic pilocarpine.[42,43] Extracellular ATP is increased after seizures[48] and P2X7R antagonists have been reported to produce antiepileptic effects,[4,44,49] which further has attracted interest for P2X7R being a tentative drug target for epilepsy.[4,44−47]

The present study finds no correlation between the disease duration and P2X7R binding levels in the temporal cortex, which is in accordance with a recent report measuring mRNA expression levels in the same tissue.[40] It should be noted that all epileptic patients included in the study are treatment refractory, have reached a chronic state, and the tissue is not coming from the epileptic focus. Therefore, the duration of the disease may not necessarily reflect any progression in disease and pathology as epileptogenesis may no longer occur. All the tissues examined here were resections, so it has not been possible to compare them to controls. Further studies in animals and in patients with epilepsy as well as in other diseases are needed to identify spatial and temporal changes in P2X7R binding.

Notably, we find no correlation between P2X7R binding and gender or age, which is in agreement with a recent study reporting the correlation to P2X7 mRNA expressions in temporal cortex resected from TLE patients.[40]

At present, TSPO PET is a widely used surrogate marker for glial cell density and neuroinflammation, and this protein is expressed in microglia and oligodendrocytes and not neurons.[16] To examine the relationship between P2X7R and TSPO, adjacent sections were incubated with [^{3}H]JNJ-64413739 and [^{123}I]CLINDE, respectively, and exposed for autoradiography. Considering the expression of P2X7R and TSPO on immune cells, a positive correlation between the binding of the two radioligands would have been expected. On the contrary, although not statistically significant, we observed an inverse correlation between P2X7R and TSPO binding. A possible explanation of these findings could be that P2X7R and TSPO have differential expression in CNS immune cells, or their regulation in response to inflammation is different or even opposite. P2X7R has been shown to be upregulated at the protein level in three samples of the temporal cortex from patients with TLE compared to the postmortem control,[8] and this upregulation of P2X7R immunoreactivity was not occurring in cells expressing microglia or astrocyte markers,[8] but localized to the presynaptic vesicle glycoprotein synaptophysin.[39,40] Immunoblotting further revealed this upregulation to be prominent in the synaptic fraction.[39] The third possibility for the observed variability could be related to variability in the focal epileptic state prior to the surgical resection of tissue. Further studies using specific markers of glial cells should be performed in order to understand the relative expression of TSPO and P2X7R on either cell types.

In conclusion, the confirmation of high binding affinity of [^{3}H]JNJ-64413739 to P2X7R in the human brain tissues further supports the potential use of the radioligand as a valuable tool to study neuroinflammation ex vivo and in vivo.

MATERIALS AND METHODS

Human Brain Tissues. Human neocortex samples were obtained from 48 drug-resistant temporal lobe epilepsy patients (24 males; 24 females) undergoing temporal lobe resection at the Rigshospitalet in Copenhagen. The average age at surgery was 41 ± 13 years, and the duration of epilepsy was 26 ± 16 years in the patient group. The outer temporal neocortex tissue consisting of both the overlying gray zone and the underlying white matter is removed in one piece in order to reach the epileptic zone underneath. Parts of this tissue were as a routine clinical procedure exposed for histopathological examination. The collected tissue was briefly washed after removal and transported to the laboratory, immediately frozen, and stored at −80 °C until further processing. The study was approved by the Ethical Committee in the Capital Region of Denmark (H-2-2011-104), and written informed consent was obtained from all patients before surgery.

The frozen tissues were sectioned in 20 μm in a CryoStar NX70 cryostat, thaw-mounted on Super-Frost Plus glass slides, and dried at room temperature, before they were stored at −80 °C for a few days before use.

Radioligands and Compounds. [^{3}H]JNJ-64413739 ((*S*)-[^{3}H](3-fluoro-2-(trifluoromethyl)pyridin-4-yl)(6-methyl-1-(pyrimidin-2-yl)-1,4,6,7-tetrahydro-5*H*-[1,2,3]triazolo[4,5-*c*]pyridin-5-yl)-methanone) was synthesized at Tritec (Switzerland). The starting material (2.2 mg) (JNJ-64413739, H. Lundbeck A/S) and 4.58 mg of the Rh(0) catalyst were suspended in 0.3 mL of tetrahydrofuran and put under an atmosphere of tritium (756 mbar, 99% gas generated from uranium oxide). The mixture was stirred at room temperature for 55 min. Subsequently, labile tritium was exchanged, and the catalyst was removed by membrane filtration. A fraction of the crude compound was purified by medium pressure liquid chromatography using the following conditions: Waters Sunfire C18, 10 × 250 mm; solvents A: water +0.1% TFA; B: acetonitrile +0.1% TFA; isocratic 54% B; 4.7 mL/min; 25 °C. The target molecule was eluted between 4.8−5.1 min. The compound was isolated from the eluent by solid phase extraction to give a batch of 8 mCi in 8 mL of ethanol with a purity of >99%. The specific activity was determined to be 81.4 Ci/mmol (3012 GBq/mmol).

The ligands used for the displacement of [^{3}H]JNJ-64413739 were apart from the cold ligand itself, also JNJ-47965567 and Lu AF27139.[28] [^{123}I]CLINDE (2-(6-chloro-2-(4-[^{123}I]iodophenyl)-imidazo[1,2-*a*]pyridin-3-yl)-*N*,*N*-diethylacetamide) was synthesized at MAP Medical Technologies (Tikkakoski, Finland) by radio-iodination by oxidation from a tin derivative and purified by reverse-

https://doi.org/10.1021/acschemneuro.2c00561
ACS Chem. Neurosci. 2023, 14, 111−118

phase high-performance liquid chromatography (HPLC). The ligand was stored in ethanol with a specific activity of 2200 Ci/mmol. [^{3}H]UCB-J ((*R*)-1-((3-[^{3}H]methylpyridin-4-yl)methyl)-4-(3,4,5-trifluorophenyl)pyrrolidin-2-one) was synthesized at Quotient Bioresearch Ltd. (United Kingdom) and provided by UCB (Braine l'Alleud, Belgium). The radiochemical concentration was 1 mCi/mL on the day of synthesis, and the specific activity of the radioligand was 24 Ci/mmol.

The specific activity left on the day of the experiment was determined for all experiments.

Autoradiography Method for [^{3}H]JNJ-64413739. Slides were allowed to reach room temperature and then preincubated in buffer (50 mM Tris−HCl, 0.5% bovine serum albumin (BSA), pH 7.4) twice for 10 min. Slides were then incubated for 2 h under constant shaking in buffer (50 mM Tris−HCl, 0.5% bovine serum albumin (BSA), 5 mM $MgCl_2$, 2 mM EGTA) with [^{3}H]JNJ-64413739.

For the saturation study, duplicate sections from one individual were incubated in concentrations spanning from 1 to 100 nM of the radioligand, and nonspecific binding was in the saturation experiment determined in the presence of 5 μM JNJ-47965567. For the displacement study, 30 nM [^{3}H]JNJ-64413739 was mixed with either the cold ligand itself or with JNJ-47965567 or Lu AF27139. The concentrations used for the displacement study ranged from 3 nM to 10 μM for all compounds.

For all autoradiography experiments with [^{3}H]JNJ-64413739, slides were washed for 3 × 5 min with ice-cold preincubation buffer followed by a quick dip in ice-cold distilled water, air-dried, and placed overnight in a paraformaldehyde vapor chamber at 4 °C. After fixation, the glass slides were kept in a silica gel desiccator for 45 min to remove any leftover moisture before exposing them to the imaging plate. Then, glass slides were put together with tritium standards ([^{3}H]microscale ART0123 (0−489.1 nCi/mg) and ART0123B (3−109.4 nCi/mg) American Radiolabeled Chemicals, Inc., St. Louis, USA) in a radiation-shielded imaging plate cassette (Fuji casette2 BAS-TR 2040, Fujifilm, Tokyo, Japan) with a tritium-sensitive imaging plate (Fuji IP BAS-TR 2040, Fujifilm, Tokyo, Japan) The glass slides were exposed to image plates overnight at 4 °C. After exposure, the imaging plate was then scanned using the Amersham Typhoon IP Biomolecular Imager (GE healthcare, Chicago, USA) at a pixel size of 25 μm.

Comparative Analysis in Multiple Human Samples. Similar series of adjacent sections mounted on individual glasses were selected for autoradiography. Glass slides, each representing adjacent sections from cortical tissue specimens from each of the 48 individuals, were incubated together with either 30 nM [^{3}H]JNJ-64413739, 0.3 nM [^{123}I]CLINDE, or 3 nM [^{3}H]UCB-J. For [^{123}I]CLINDE and [^{3}H]UCB-J, the autoradiography was conducted as earlier described[29,30] and used as a tool for delineation of the gray matter.

The sections were exposed to image plates together with standards overnight for [^{3}H]JNJ-64413739 and [^{3}H]UCB-J, but only for 10 min for [^{123}I]CLINDE. After exposure, the image plates were scanned using the Amersham Typhoon IP Biomolecular Imager.

Data Analysis and Statistics. Quantitative analysis of receptor binding in cortex slices was performed by measuring the mean of optical density (OD) in the region of interest (ROI). These ROIs were either gray matter that was identified by the guidance from similar autoradiography for SV2A, a marker only expressed in neurons,[31] or white matter defined as the remaining tissue area (see Figure 1). For CLINDE, the entire section was used for analysis. The gray values from tritium standards were used to interpolate the gray values from the ROI in cortical regions to obtain radioactivity values using the Image J Rodbard (NIH Image) curve. The decay-corrected specific activity of the radioligand is used to convert binding values (fmol/mg TE). Specific binding was defined as total binding from which nonspecific binding was obtained by coincubating with the surplus of JNJ-47965567 in an adjacent section.

Statistical analysis from autoradiography data calculation was performed using the nonlinear regression function program of Graphpad Prism (version 9.2.0; GraphPad Software, San Diego, USA). Data points on graphs are expressed as mean ± standard deviation.

AUTHOR INFORMATION

Corresponding Author

Jens D. Mikkelsen − *Neurobiology Research Unit, University Hospital Rigshospitalet, Copenhagen 2100, Denmark; Institute of Neuroscience, University of Copenhagen, Copenhagen 2200, Denmark; Department of Molecular Medicine, University of Southern Denmark, Odense 5000, Denmark;* orcid.org/0000-0001-9824-7359; Phone: +45 3545 6701; Email: jens.mikkelsen@sund.ku.dk

Authors

Sanjay S. Aripaka − *Neurobiology Research Unit, University Hospital Rigshospitalet, Copenhagen 2100, Denmark*

Sif Kaad − *Neurobiology Research Unit, University Hospital Rigshospitalet, Copenhagen 2100, Denmark*

Burcu A. Pazarlar − *Neurobiology Research Unit, University Hospital Rigshospitalet, Copenhagen 2100, Denmark; Physiology Department, Faculty of Medicine, Izmir Katip Celebi University, Izmir 35330, Turkey*

Lars Pinborg − *Neurobiology Research Unit, University Hospital Rigshospitalet, Copenhagen 2100, Denmark; Epilepsy Clinic, Department of Neurology, Copenhagen University Hospital, Copenhagen 2100, Denmark*

Bente Finsen − *Department of Molecular Medicine, University of Southern Denmark, Odense 5000, Denmark*

Andrea Varrone − *H. Lundbeck A/S, Valby 2500, Denmark*

Benny Bang-Andersen − *H. Lundbeck A/S, Valby 2500, Denmark*

Jesper F. Bastlund − *H. Lundbeck A/S, Valby 2500, Denmark*

Complete contact information is available at: https://pubs.acs.org/10.1021/acschemneuro.2c00561

Author Contributions

J.D.M. and J.F.B. designed the experiments. B.B.-A., A.V., and L.P. provided materials and tissues. S.S.A., S.K., and B.A.P. conducted the experiments and J.D.M., B.F., S.S.A., S.K., and B.A.P. analyzed the data. All authors read and provided comments to an earlier draft of the manuscript and approved the final version.

Notes

The authors declare no competing financial interest.

ACKNOWLEDGMENTS

UCB Pharma is thanked for providing [^{3}H]UCB-J.

REFERENCES

(1) Bhattacharya, A.; Biber, K. The microglial ATP-gated ion channel P2X7 as a CNS drug target. *Glia* **2016**, *64*, 1772−1787.

(2) Sperlagh, B.; Illes, P. P2X7 receptor: an emerging target in central nervous system diseases. *Trends Pharmacol. Sci.* **2014**, *35*, 537−547.

(3) Andrejew, R.; Oliveira-Giacomelli, A.; Ribeiro, D. E.; et al. The P2X7 Receptor: Central Hub of Brain Diseases. *Front. Mol. Neurosci.* **2020**, *13*, 124.

(4) Gil, B.; Smith, J.; Tang, Y.; et al. Beyond Seizure Control: Treating Comorbidities in Epilepsy via Targeting of the P2X7 Receptor. *Int. J. Mol. Sci.* **2022**, *23*, 2380.

(5) Matute, C.; Torre, I.; Perez-Cerda, F.; et al. P2X(7) receptor blockade prevents ATP excitotoxicity in oligodendrocytes and

ameliorates experimental autoimmune encephalomyelitis. *J. Neurosci.* **2007**, *27*, 9525−9533.
(6) Illes, P.; Khan, T. M.; Rubini, P. Neuronal P2X7 Receptors Revisited: Do They Really Exist? *J. Neurosci.* **2017**, *37*, 7049−7062.
(7) Miras-Portugal, M. T.; Sebastian-Serrano, A.; de Diego, G. L.; et al. Neuronal P2X7 Receptor: Involvement in Neuronal Physiology and Pathology. *J. Neurosci.* **2017**, *37*, 7063−7072.
(8) Jimenez-Pacheco, A.; Mesuret, G.; Sanz-Rodriguez, A.; et al. Increased neocortical expression of the P2X7 receptor after status epilepticus and anticonvulsant effect of P2X7 receptor antagonist A-438079. *Epilepsia* **2013**, *54*, 1551−1561.
(9) Leon, D.; Sanchez-Nogueiro, J.; Marin-Garcia, P.; et al. Glutamate release and synapsin-I phosphorylation induced by P2X7 receptors activation in cerebellar granule neurons. *Neurochem. Int.* **2008**, *52*, 1148−1159.
(10) Rigato, C.; Swinnen, N.; Buckinx, R.; et al. Microglia proliferation is controlled by P2X7 receptors in a Pannexin-1-independent manner during early embryonic spinal cord invasion. *J. Neurosci.* **2012**, *32*, 11559−11573.
(11) Sanz, J. M.; Chiozzi, P.; Ferrari, D.; et al. Activation of microglia by amyloid {beta} requires P2X7 receptor expression. *J. Immunol.* **2009**, *182*, 4378−4385.
(12) Martinez-Frailes, C.; Di Lauro, C.; Bianchi, C.; et al. Amyloid Peptide Induced Neuroinflammation Increases the P2X7 Receptor Expression in Microglial Cells, Impacting on Its Functionality. *Front. Cell Neurosci.* **2019**, *13*, 143.
(13) Ferrari, D.; Pizzirani, C.; Adinolfi, E.; et al. The P2X7 receptor: a key player in IL-1 processing and release. *J. Immunol.* **2006**, *176*, 3877−3883.
(14) He, Y.; Taylor, N.; Fourgeaud, L.; et al. The role of microglial P2X7: modulation of cell death and cytokine release. *J. Neuroinflammation* **2017**, *14*, 135.
(15) Kreisl, W. C.; Kim, M. J.; Coughlin, J. M.; et al. PET imaging of neuroinflammation in neurological disorders. *Lancet Neurol.* **2020**, *19*, 940−950.
(16) De Picker, L. J.; Haarman, B. C. M. Applicability, potential and limitations of TSPO PET imaging as a clinical immunopsychiatry biomarker. *Eur. J. Nucl. Med. Mol. Imaging* **2021**, *49*, 164−173.
(17) Territo, P. R.; Meyer, J. A.; Peters, J. S.; et al. Characterization of (11)C-GSK1482160 for Targeting the P2X7 Receptor as a Biomarker for Neuroinflammation. *J. Nucl. Med.* **2017**, *58*, 458−465.
(18) Ory, D.; Celen, S.; Gijsbers, R.; et al. Preclinical Evaluation of a P2X7 Receptor-Selective Radiotracer: PET Studies in a Rat Model with Local Overexpression of the Human P2X7 Receptor and in Nonhuman Primates. *J. Nucl. Med.* **2016**, *57*, 1436−1441.
(19) Berdyyeva, T.; Xia, C.; Taylor, N.; et al. PET Imaging of the P2X7 Ion Channel with a Novel Tracer [(18)F]JNJ-64413739 in a Rat Model of Neuroinflammation. *Mol. Imaging Biol.* **2019**, *21*, 871−878.
(20) Kolb, H. C.; Barret, O.; Bhattacharya, A.; et al. Preclinical Evaluation and Nonhuman Primate Receptor Occupancy Study of (18)F-JNJ-64413739, a PET Radioligand for P2X7 Receptors. *J. Nucl. Med.* **2019**, *60*, 1154−1159.
(21) Koole, M.; Schmidt, M. E.; Hijzen, A.; et al. (18)F-JNJ-64413739, a Novel PET Ligand for the P2X7 Ion Channel: Radiation Dosimetry, Kinetic Modeling, Test-Retest Variability, and Occupancy of the P2X7 Antagonist JNJ-54175446. *J. Nucl. Med.* **2019**, *60*, 683−690.
(22) Mertens, N.; Schmidt, M. E.; Hijzen, A.; et al. Minimally invasive quantification of cerebral P2X7R occupancy using dynamic [(18)F]JNJ-64413739 PET and MRA-driven image derived input function. *Sci. Rep.* **2021**, *11*, 16172.
(23) Fantoni, E. R.; Dal Ben, D.; Falzoni, S.; et al. Design, synthesis and evaluation in an LPS rodent model of neuroinflammation of a novel (18)F-labelled PET tracer targeting P2X7. *EJNMMI Res.* **2017**, *7*, 31.
(24) Fu, Z.; Lin, Q.; Hu, B.; et al. P2X7 PET Radioligand (18)F-PTTP for Differentiation of Lung Tumor from Inflammation. *J. Nucl. Med.* **2019**, *60*, 930−936.
(25) Van Weehaeghe, D.; Koole, M.; Schmidt, M. E.; et al. [(11)C]JNJ54173717, a novel P2X7 receptor radioligand as marker for neuroinflammation: human biodistribution, dosimetry, brain kinetic modelling and quantification of brain P2X7 receptors in patients with Parkinson's disease and healthy volunteers. *Eur. J. Nucl. Med. Mol. Imaging* **2019**, *46*, 2051−2064.
(26) Van Weehaeghe, D.; Van Schoor, E.; De Vocht, J.; et al. TSPO Versus P2X7 as a Target for Neuroinflammation: An In Vitro and In Vivo Study. *J. Nucl. Med.* **2020**, *61*, 604−607.
(27) Hagens, M. H. J.; Golla, S. S. V.; Janssen, B.; et al. The P2X7 receptor tracer [(11)C]SMW139 as an in vivo marker of neuroinflammation in multiple sclerosis: a first-in man study. *Eur. J. Nucl. Med. Mol. Imaging* **2020**, *47*, 379−389.
(28) Hopper, A. T.; Juhl, M.; Hornberg, J.; et al. Synthesis and Characterization of the Novel Rodent-Active and CNS-Penetrant P2X7 Receptor Antagonist Lu AF27139. *J. Med. Chem.* **2021**, *64*, 4891−4902.
(29) Donat, C. K.; Gaber, K.; Meixensberger, J.; et al. Changes in Binding of [(123)I]CLINDE, a High-Affinity Translocator Protein 18 kDa (TSPO) Selective Radioligand in a Rat Model of Traumatic Brain Injury. *NeuroMol. Med.* **2016**, *18*, 158−169.
(30) Metaxas, A.; Thygesen, C.; Briting, S. R. R.; et al. Increased Inflammation and Unchanged Density of Synaptic Vesicle Glycoprotein 2A (SV2A) in the Postmortem Frontal Cortex of Alzheimer's Disease Patients. *Front. Cell Neurosci.* **2019**, *13*, 538.
(31) Pazarlar, B. A.; Aripaka, S. S.; Petukhov, V.; et al. Expression profile of synaptic vesicle glycoprotein 2A, B, and C paralogues in temporal neocortex tissue from patients with temporal lobe epilepsy (TLE). *Mol. Brain* **2022**, *15*, 45.
(32) Morgan, J.; Alves, M.; Conte, G.; et al. Characterization of the Expression of the ATP-Gated P2X7 Receptor Following Status Epilepticus and during Epilepsy Using a P2X7-EGFP Reporter Mouse. *Neurosci. Bull.* **2020**, *36*, 1242−1258.
(33) Butt, A. M.; Fern, R. F.; Matute, C. Neurotransmitter signaling in white matter. *Glia* **2014**, *62*, 1762−1779.
(34) Hamilton, N.; Vayro, S.; Kirchhoff, F.; et al. Mechanisms of ATP- and glutamate-mediated calcium signaling in white matter astrocytes. *Glia* **2008**, *56*, 734−749.
(35) Yu, Y.; Ugawa, S.; Ueda, T.; et al. Cellular localization of P2X7 receptor mRNA in the rat brain. *Brain Res.* **2008**, *1194*, 45−55.
(36) McCarthy, A. E.; Yoshioka, C.; Mansoor, S. E. Full-Length P2X7 Structures Reveal How Palmitoylation Prevents Channel Desensitization. *Cell* **2019**, *179*, 659−670.e13.
(37) Rassendren, F.; Buell, G. N.; Virginio, C.; et al. The permeabilizing ATP receptor, P2X7. Cloning and expression of a human cDNA. *J. Biol. Chem.* **1997**, *272*, 5482−5486.
(38) Cheewatrakoolpong, B.; Gilchrest, H.; Anthes, J. C.; et al. Identification and characterization of splice variants of the human P2X7 ATP channel. *Biochem. Biophys. Res. Commun.* **2005**, *332*, 17−27.
(39) Barros-Barbosa, A. R.; Fonseca, A. L.; Guerra-Gomes, S.; et al. Up-regulation of P2X7 receptor-mediated inhibition of GABA uptake by nerve terminals of the human epileptic neocortex. *Epilepsia* **2016**, *57*, 99−110.
(40) Guerra Leal, B.; Barros-Barbosa, A.; Ferreirinha, F.; et al. Mesial Temporal Lobe Epilepsy (MTLE) Drug-Refractoriness Is Associated With P2X7 Receptors Overexpression in the Human Hippocampus and Temporal Neocortex and May Be Predicted by Low Circulating Levels of miR-22. *Front. Cell Neurosci.* **2022**, *16*, No. 910662.
(41) Engel, T.; Gomez-Villafuertes, R.; Tanaka, K.; et al. Seizure suppression and neuroprotection by targeting the purinergic P2X7 receptor during status epilepticus in mice. *FASEB J.* **2012**, *26*, 1616−1628.
(42) Dona, F.; Ulrich, H.; Persike, D. S.; et al. Alteration of purinergic P2X4 and P2X7 receptor expression in rats with temporal-lobe epilepsy induced by pilocarpine. *Epilepsy Res.* **2009**, *83*, 157−167.
(43) Hong, S.; Xin, Y.; JiaWen, W.; et al. The P2X7 receptor in activated microglia promotes depression- and anxiety-like behaviors in

https://doi.org/10.1021/acschemneuro.2c00561
ACS Chem. Neurosci. 2023, 14, 111−118

lithium -pilocarpine induced epileptic rats. *Neurochem. Int.* **2020**, *138*, No. 104773.
(44) Beamer, E.; Fischer, W.; Engel, T. The ATP-Gated P2X7 Receptor As a Target for the Treatment of Drug-Resistant Epilepsy. *Front. Neurosci.* **2017**, *11*, 21.
(45) Beamer, E.; Kuchukulla, M.; Boison, D.; et al. ATP and adenosine-Two players in the control of seizures and epilepsy development. *Prog. Neurobiol.* **2021**, *204*, No. 102105.
(46) Engel, T.; Alves, M.; Sheedy, C.; et al. ATPergic signalling during seizures and epilepsy. *Neuropharmacology* **2016**, *104*, 140−153.
(47) Rassendren, F.; Audinat, E. Purinergic signaling in epilepsy. *J. Neurosci. Res.* **2016**, *94*, 781−793.
(48) Klaft, Z. J.; Schulz, S. B.; Maslarova, A.; et al. Extracellular ATP differentially affects epileptiform activity via purinergic P2X7 and adenosine A1 receptors in naive and chronic epileptic rats. *Epilepsia* **2012**, *53*, 1978−1986.
(49) Engel, T.; Nicke, A.; Deussing, J. M.; et al. Editorial: P2X7 as Common Therapeutic Target in Brain Diseases. *Front. Mol. Neurosci.* **2021**, *14*, No. 656011.

https://doi.org/10.1021/acschemneuro.2c00561
ACS Chem. Neurosci. 2023, 14, 111−118